

Article

Ferroelectricity, Superconductivity, and SrTiO₃—Passions of K.A. Müller

Gernot Scheerer, Margherita Boselli, Dorota Pulmannova, Carl Willem Rischau , Adrien Waelchli, Stefano Gariglio, Enrico Giannini , Dirk van der Marel  and Jean-Marc Triscone *

Department of Quantum Matter Physics, University of Geneva, 24 Quai Ernest-Ansermet, 1211 Geneva 4, Switzerland; gernot.scheerer@unige.ch (G.S.); margherita.boselli@unige.ch (M.B.); Dorota.Pulmannova@unige.ch (D.P.); Willem.Rischau@unige.ch (C.W.R.); Adrien.Waelchli@unige.ch (A.W.); stefano.gariglio@unige.ch (S.G.); enrico.giannini@unige.ch (E.G.); Dirk.VanDerMarel@unige.ch (D.v.d.M.)

* Correspondence: Jean-Marc.Triscone@unige.ch

Received: 9 September 2020; Accepted: 13 October 2020; Published: 15 October 2020



Abstract: SrTiO₃ is an insulating material which, using chemical doping, pressure, strain or isotope substitution, can be turned into a ferroelectric material or into a superconductor. The material itself, and the two aforementioned phenomena, have been subjects of intensive research of Karl Alex Müller and have been a source of inspiration, among other things, for his Nobel prize-winning research on high temperature superconductivity. An intriguing outstanding question is whether the occurrence of ferroelectricity and superconductivity in the same material is just a coincidence, or whether a deeper connection exists. In addition there is the empirical question of how these two phenomena interact with each other. Here we show that it is possible to induce superconductivity in a two-dimensional layer at the interface of SrTiO₃ and LaAlO₃ when we make the SrTiO₃ ferroelectric by means of ¹⁸O substitution. Our experiments indicate that the ferroelectricity is perfectly compatible with having a superconducting two-dimensional electron system at the interface. This provides a promising avenue for manipulating superconductivity in a non centrosymmetric environment.

Keywords: ferroelectricity; superconductivity; SrTiO₃; ¹⁸O; isotope substitution; SrTiO₃/LaAlO₃; interface; heterostructure

1. Introduction

Karl Alex Müller has numerous interests and passions. Most likely quite high in the list are ferroelectricity, superconductivity and SrTiO₃—a material that, we believe, he called the drosophila of solid state physics. Known worldwide for their discovery of superconductivity in the cuprates, J.G. Bednorz and K.A. Müller explained in their Nobel lecture that their search for high T_c superconductivity in complex oxides had been partly motivated by SrTiO₃, which, once doped, has a maximum T_c of 0.5 K, actually very high when compared to its Fermi energy [1].

Close to ferroelectricity and to superconductivity, SrTiO₃ is indeed an amazing material. By itself it is an insulating cubic perovskite at room temperature. Below 105 K, an antiferrodistortive transition makes the system weakly tetragonal. Electronically, SrTiO₃ is a quantum paraelectric—a compound often seen as “failed ferroelectric” with its inverse static dielectric constant ϵ versus T revealing a Curie–Weiss behavior. Unlike for ferroelectric materials, however, ϵ never diverges but saturates at low temperatures as shown in 1979 by Müller and Burkard [2]. When doped, SrTiO₃ can be turned into a ferroelectric or into

a superconductor. To achieve the former, Ca can be partially substituted for Sr [3] or ^{16}O can be replaced by ^{18}O [4]—in thin film form, strain also allows the ferroelectric state to be reached [5]. Superconductivity can be obtained by partially substituting Sr with La, Ti with Nb or by reducing the oxygen content—in all cases, the system is doped with electrons and the maximum T_c is around 500 mK [6,7]. SrTiO_3 has, over time, revealed other amazing properties including the emission of blue-light once irradiated with Ar ions [8] or the electrolysis of water [9]. With the discovery in 2004 of conductivity [10] and in 2007 of superconductivity [11] at the interface between LaAlO_3 and SrTiO_3 , this "magic" perovskite was again at the center of worldwide attention. More recently, it is the prediction and discovery of an increase of T_c in electron-doped and Ca or ^{18}O substituted SrTiO_3 that triggered a lot of interest, discoveries marrying the passions of K.A. Müller—ferroelectricity, superconductivity and SrTiO_3 .

In this paper, we aim to discuss how the proximity of a ferroelectric state to the superconducting phase may explain the Cooper pair coupling mechanism. We first review the properties of SrTiO_3 , presenting a short summary of its phase diagram with the different ground states obtained by the various dopings and substitutions. We then recall the different models proposed since as far back as 1964 that may explain superconductivity in SrTiO_3 and we discuss in particular ideas allowing the recent observation of T_c enhancement when SrTiO_3 is pushed toward ferroelectricity to be understood. Finally, we briefly introduce the $\text{LaAlO}_3/\text{SrTiO}_3$ system and show some experimental results obtained on these superconducting interfaces for which ^{16}O was partially substituted by ^{18}O in the SrTiO_3 single crystal substrate used for the growth of the LaAlO_3 layer. We end the paper with a brief conclusion.

2. SrTiO_3 : Properties, Phase Diagram and Tuning Parameters

The centrosymmetric cubic perovskite structure (tolerance factor $t = 1$) that SrTiO_3 adopts at room temperature reflects the perfect balance between the ionic radii of its cations: deviations from $t = 1$ would lead to various types of distortions, the most common ones being the oxygen octahedral rotations occurring for $t < 1$ [12]. As mentioned above, at 105 K SrTiO_3 goes through an antiferrodistortive (AFD) transition resulting in a tetragonal structure with oxygen octahedra rotated out of phase about the c-axis ($a^0a^0c^-$ in Glazer notation) [13]. Lowering the temperature further produces a softening of the ferroelectric phonon mode with a strong Curie–Weiss type increase of the static dielectric response, suggesting a transition into a ferroelectric state at 20 K [14]. However, Müller and Burkard discovered that the dielectric constant saturates, reaching a value of 2×10^4 at 4 K [2]: they interpreted this saturation as the signature of an intrinsic quantum paraelectric state, i.e., an avoided ferroelectric state due to the quantum fluctuations of the atoms about their centrosymmetric positions. Monte Carlo calculations have confirmed this scenario and revealed the role of quantum fluctuations on the reduction of the AFD transition temperature [15]. Given such proximity to a ferroelectric state, several groups have explored different approaches to obtain a polar state, applying mechanical [16,17] and epitaxial [5] strain or performing chemical—replacing Sr with Ca [3]—or isotopic substitutions— ^{16}O with ^{18}O [4]. These different avenues have induced a ferroelectric ground state with Curie temperatures exceeding, in some cases, room temperature [5]. Figure 1 shows schematically how the ferroelectric state develops beyond the quantum critical point (QCP) for the case of Ca-doping and ^{18}O -substitution.

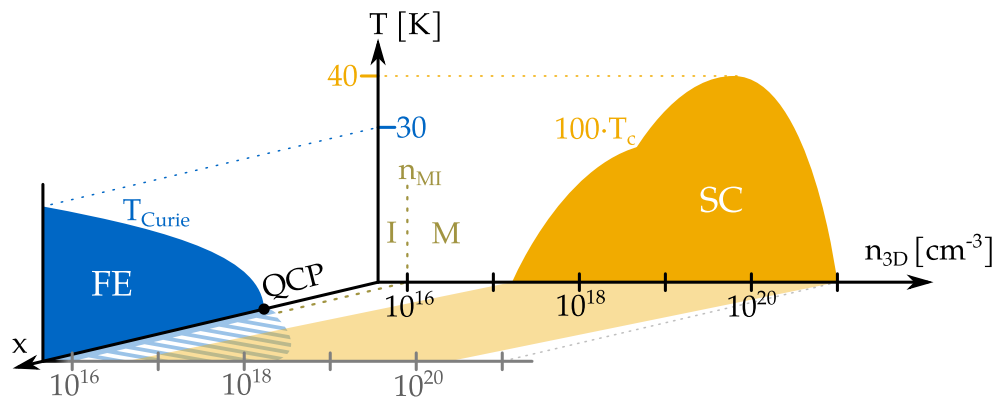


Figure 1. Schematic phase diagram of SrTiO₃ showing the ferroelectric (FE) and superconducting (SC) phases. Upon chemical substitution of Ca for Sr, i.e., Sr_{1-x}Ca_xTiO₃ with 0.002 < x < 0.02 [3], or by oxygen isotope substitution, i.e., SrTi(¹⁸O_y¹⁶O_{1-y})₃ with y > 0.33 [4], the material develops a FE ground state beyond a quantum critical point (QCP). This FE phase occurs well below the structural transition from cubic to tetragonal [18]. Charge doping turns the material from an insulator (I) into a metal (M) at a critical carrier density (n_{MI}) of 10¹⁶ cm⁻³, while SC develops in a doping range n_{3D} between 5 × 10¹⁷ and 10²¹ cm⁻³.

The large dielectric susceptibility is thought to be responsible for the fact that the electronic transition from the insulating state to a metallic state occurs at an extremely low carrier density of 10¹⁶ cm⁻³ [19]. Such doping can be induced by chemical substitution of La for Sr [20], Nb for Ti or by oxygen reduction [21]. At these low dopings the mean free path of the conduction electrons is about 100 times greater than the Fermi wavelength [22]. One of the consequences is that quantum oscillations in the magneto-resistance are observed [23,24], a feature that allows the topology of the Fermi surface to be determined as a function of carrier density. At low temperatures (below 0.4 K), the metallic electron doped system undergoes a phase transition into a superconducting condensate for a carrier density in the range 10¹⁷–10²¹ cm⁻³ [24–26]. With 10¹⁷ cm⁻³, doped SrTiO₃ is the lowest density superconductor and displays a unique broad range of charge concentration over which the superconducting state is observed. The origin of the superconducting state and the dependence of the superconducting temperature on carrier density have been subjects of several studies [26,27]. An appealing proposition is that the two different order parameters may be somehow coupled: according to certain models that apply to perovskite-type structures, the ferroelectric instability is the condition necessary to pair electrons [28]. Such an idea has been explored recently, leading to a clear prediction of the dependence of the superconducting critical temperature upon the proximity to the ferroelectric state [29].

3. Superconductivity in Doped SrTiO₃ from 1964 until 2020

Using the linear combination of atomic orbitals method, Kahn and Leyendecker predicted in 1964 that the electronic energy bands in strontium titanate exhibit six conduction band ellipsoids lying along [100] directions of momentum space with minima probably at the edges of the Brillouin zone [30]. In the same year, Marvin Cohen predicted that the attractive electron–electron interaction arising from the exchange of intravalley and intervalley phonons can cause these materials to exhibit superconducting properties [31]. In less than a year, Schooley et al. [6,25] reported superconductivity in electron-doped SrTiO₃ with carrier concentrations in the range from 10¹⁸ to 10²¹ cm⁻³, and T_c ranging from 50 mK at the lowest doping to about 0.5 K for n_c = 10²⁰ cm⁻³. While these results confirmed Cohen’s prediction of superconductivity in electron-doped SrTiO₃, it has been demonstrated by later band structure calculations [32] that there is only a single valley, which is located at the Brillouin zone center for each of the three conduction bands.

The three bands at the zone center are non-degenerate due to spin-orbit splitting and (below 105 K) a weak tetragonal crystal field [22], causing the sudden onset of quantum oscillations [23] at the critical dopings where the second and third band become occupied [24]. This also agrees well with the doping dependence of the two superconducting gaps observed by Binnig et al. [33]. While the Fermi surface properties agree well with the ab initio band structure predictions, the experimental values of the effective mass are a factor of two higher than the ab initio predictions [34,35]. From the analysis of the mid-infrared absorption in doped SrTiO₃ it has become clear that the factor of two for the mass enhancement observed in the experiments is a consequence of the coupling of the conduction electrons to the longitudinal optical phonons, and that the mid-infrared peaks originate from large polaron formation [36].

In the course of the more than five decades of research on SrTiO₃ a variety of models have been proposed for the pairing mechanism: intervalley scattering [27,31], bipolarons [37], two-phonon exchange [38], longitudinal optical phonons [39], full dielectric function for longitudinal phonons and screened Coulomb [40,41], acoustic phonons [42]. A possible role of ferroelectricity was proposed by Bussmann-Holder [28], an idea that has gained momentum in recent years [43]. A detailed theoretical prediction of a giant isotope effect on the superconducting T_c [29] with an opposite sign from the BCS prediction has spurred on a number of isotope-substitution experiments [44,45] and Ca-substitution experiments, which are expected to have a similar effect on T_c [46]. These experiments have confirmed the theoretical predictions. The theory was based on the coupling of electrons to the soft transverse optical phonon (the “TO1” mode). A problem has meanwhile been pointed out, that the coupling to this phonon is far too small to account for T_c on the order of several hundred mK [47]. A possible remedy is to couple the electrons to pairs of transverse optical phonons of opposite momentum [38,48]. A recent analysis of the optical oscillator strength of the TO1 mode has brought to light that this type of bi-phonon exchange is indeed unusually strong in SrTiO₃ [49], strong enough in fact to account for superconductivity in this material. In this scenario quantum ferroelectric fluctuations induce the pairing interaction that leads to superconductivity [29,43]; however, the main channel of interaction is mediated by pairs of phonons rather than single phonons as was originally proposed. In this context it is not an accident that superconductivity occurs in proximity to a ferroelectric quantum critical point.

4. Superconductivity in Two Dimensions

Recent research on SrTiO₃ has focused on the two-dimensional electron systems that emerge at the crystal surface or in thin films. Mobile electrons can be localized at the surface of undoped SrTiO₃ crystals by cleaving in vacuum [50,51], in δ -doped SrTiO₃ thin films [52] or in SrTiO₃-based heterostructures. The well-known conducting interface between an insulating SrTiO₃ substrate and a thin film of LaAlO₃ belongs to the last class [10]. This heterostructure hosts a two-dimensional conducting system confined in SrTiO₃ within a few nanometers from its interface with LaAlO₃. The electrons are transferred to SrTiO₃ to compensate for the polar discontinuity occurring between the two materials along the [001] direction [53–55]. Similar to the bulk case, this system undergoes a superconducting transition when cooled down below 300 mK. As-grown samples have a critical temperature of ~ 200 mK, and a 1D critical current density of $100 \mu\text{A}/\text{cm}$ [11]. The superconductivity in this system has a two-dimensional character. Indeed, the analysis of the critical magnetic field parallel, H_{\parallel}^* , and perpendicular, H_{\perp}^* , to the interface yields a Ginzburg–Landau coherence length, ξ , of 60 nm at $T = 0$ K, and a thickness of the superconducting slab of 11 nm. As expected for a superconducting thin film (thickness $\ll \xi$) [56], H_{\parallel}^* is much higher than H_{\perp}^* as a 2D superconducting layer cannot accommodate a vortex parallel to the plane. Interestingly, the value of H_{\parallel}^* exceeds the paramagnetic limit set by BCS theory, $\mu_0 \cdot H_{\parallel}^* = 1.84 \cdot T_c$ (with $\mu_0 \cdot H_{\parallel}^*$ in T and T_c in K), by a factor of 4–5 [57], and this effect might be linked to the presence of strong spin-orbit coupling in the system [58,59].

In 2008, Caviglia et al. showed that the superconductivity is tunable by the electric field effect [60]. The phase diagram of LaAlO₃/SrTiO₃ resembles that of bulk SrTiO₃, but it extends over a much smaller carrier density range, between $1 \times 10^{19} \text{ cm}^{-3}$ and $4 \times 10^{19} \text{ cm}^{-3}$ [61]. In the underdoped region of the phase diagram, a quantum critical point separates the superconducting regime from an insulating phase, related to the weak-localization effect [60].

5. ¹⁸O Isotope Effect

Following the ferroelectric quantum critical scenario proposed by Rowley et al. [43], Edge et al. considered a specific scenario in which the ferroelectric soft mode is tuned by isotopic ¹⁸O-substitution [29]. By tuning the ¹⁸O substitution level beyond the QCP, they predicted both an increase of the maximum T_c and a shift of the maximum of the dome to lower carrier densities. Experimentally, the increase of T_c was first observed by Stucky et al. on 35%-isotope substituted samples that were electron-doped by oxygen removal [44]. In the BCS weak-coupling limit, T_c is inversely proportional to the isotope mass M : $T_c \propto M^{-\alpha}$ with an isotope coefficient $\alpha = +0.5$. The experimentally determined increase of T_c of 50% [44] leads, however, to a negative and much larger value of $\alpha \approx -10$, matching the theoretical prediction made by Edge and coworkers, both in sign and order of magnitude [29]. In a later work an enhancement of T_c upon isotope substitution was further confirmed in isotope-substituted samples that were electron-doped by substituting Sr with La [45].

In this context, we measured the electronic properties of LaAlO₃/SrTi(¹⁸O_{*y*}¹⁶O_{1-*y*})₃ heterostructures: a system where a superconducting two-dimensional electron system is confined at the interface between an insulating thin film and a ferroelectric substrate.

We optimized the isotopic substitution on commercial TiO₂ terminated SrTiO₃ substrates provided by CrysTec GmbH. Several crystals, $5 \times 2.5 \times 0.5 \text{ mm}^3$ and $5 \times 2.5 \times 0.25 \text{ mm}^3$ in size, are put in a standard quartz tube, which is then sealed to fix the internal pressure of ¹⁸O₂ at 0.4–0.7 bar. The sealed tubes are placed in a tube furnace and heated up at temperatures between 700 and 1100 °C for 20–40 days. Before the LaAlO₃ thin film growth, we evaluated the effect of the substitution procedure on the substrate topography using an atomic force microscope (AFM).

As-received TiO₂ terminated substrates have an atomically flat surface with a clear step-and-terrace topography (see Figure 2a). AFM imaging revealed that after the thermal treatment the crystal surface is completely reconstructed. Instead of the usual step-and-terrace structure, we found a “block-terrace” structure (see Figure 2b). In order to restore a controlled TiO₂ termination, the crystals have been re-polished and then treated in an HF (hydrofluoric acid) bath for 30 s, followed by a rinsing with demineralized water. After this procedure, the substrates recovered the initial step-terrace structure (see Figure 2c), with atomically flat terraces and unit cell-high steps, and were ready for the LaAlO₃ deposition. The thin films of LaAlO₃ were grown by pulsed laser deposition, following the recipe used for standard LaAlO₃/SrTiO₃ heterostructures [62]. Their thickness, typically 6–7 unit cells, was monitored during the growth using reflection high energy electron diffraction (see Figure 2d). After the growth, a 20 nm gold layer was sputtered on the back side of the substrate to be used as an electrode for dielectric measurements.

We prepared and analyzed three LaAlO₃/SrTi(¹⁸O_{*y*}¹⁶O_{1-*y*})₃ heterostructures with nominal ¹⁸O contents in the SrTiO₃ substrate of 35%, 45%, and 67%, respectively. Compared to pure SrTiO₃, the low-temperature dielectric constant, ϵ_r , is strongly enhanced by the presence of ¹⁸O (see Figure 2e). At $y = 35\%$ the substrate is on the verge of the ferroelectric transition and ϵ_r saturates at roughly 4.7×10^4 (compared to 2×10^4 for SrTiO₃). For $y = 45\%$ and 67% , the dielectric constant has a double peak structure, with the maxima indicating the position of the ferroelectric transition. The first peak occurs approximately at the Curie temperature of 12 K (17 K), which agrees well with the nominal ¹⁸O content 45% (67%),

as indicated by the black arrow in Figure 2e. The second peak, which occurs at lower temperature (gray arrows), may be due to inhomogeneities in the ^{18}O content. It is worth noting that the substrates are heated up to $800\text{ }^\circ\text{C}$ in an ^{16}O atmosphere during the growth of the LaAlO_3 film [62] and some ^{16}O may re-substitute part of the ^{18}O present at the SrTiO_3 surface. The second peak is visible at 6.9 K (8.1 K) and corresponds to an ^{18}O content of roughly 35% (40%) for a nominal content of 45% (67%).

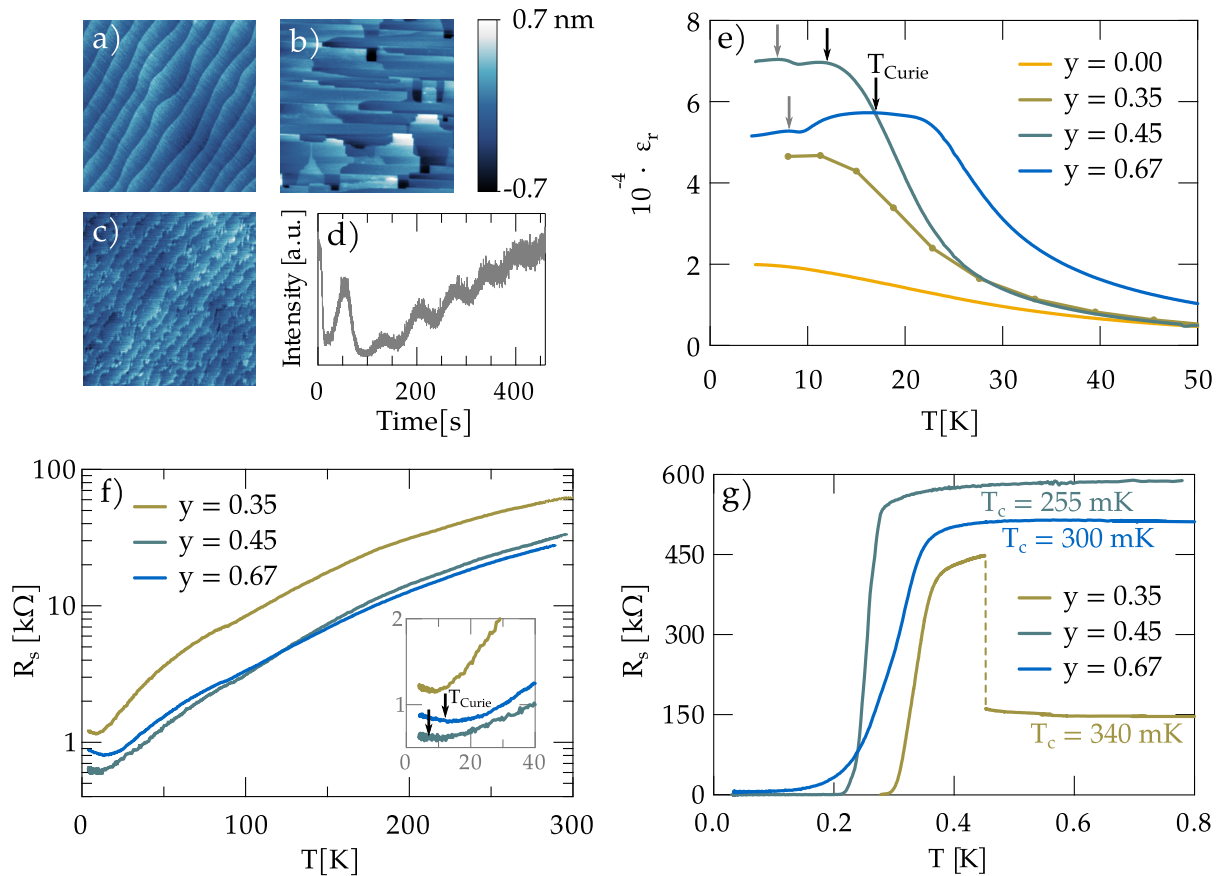


Figure 2. Growth and physical properties of $\text{LaAlO}_3/\text{SrTi}({}^{18}\text{O}_y\text{O}_{1-y})_3$ interfaces. AFM images of the SrTiO_3 substrate (a) as-received, (b) after the $^{18}\text{O}_y$ substitution process, and (c) after re-polishing and HF treatment (the size of all AFM images is $4\text{ }\mu\text{m} \times 4\text{ }\mu\text{m}$). (d) RHEED signal during the growth of the LaAlO_3 layer. One oscillation corresponds to the deposition of one unit cell of LaAlO_3 . (e) Dielectric constant versus temperature of a SrTiO_3 substrate ($y = 0$) and of $\text{LaAlO}_3/\text{SrTi}({}^{18}\text{O}_y\text{O}_{1-y})_3$ samples for different values of substitution. The dielectric properties have been measured in a homemade Helium cryostat using the Agilent E4980A Precision LCR Meter. The electric field was applied between the back electrode and the 2DES used as a top-electrode. (f,g) Sheet resistance versus temperature of the 2D electron system for ^{18}O substituted samples. The resistance jump visible in the curve for $y = 35\%$ at $\sim 0.45\text{ K}$ is due to an electric spike, which occurred in the measurement system during our study.

Figure 2f,g shows the sheet resistance (R_s) as a function of temperature. Between 300 and 1.5 K , the behavior of these samples is similar to that of standard $\text{LaAlO}_3/\text{SrTiO}_3$ heterostructures [63]. The resistance has a slight dip at $\sim 95\text{ K}$, which is presumably due to the antiferrodistortive transition at 105 K [64–66]. For all investigated samples, the resistance shows a small upturn below $\sim 15\text{ K}$, the origin of which is still under investigation. It should be noted that an anomaly/upturn has been

observed in the low-temperature resistivity of bulk Ca-substituted $\text{SrTiO}_{3-\delta}$ samples and was associated to a ferroelectric-like state still existing in metallic samples [46,67]. Similarly, a study performed on heterostructures of LaAlO_3 grown on top of Ca-substituted SrTiO_3 substrates showed the presence of a resistance upturn occurring just below the Curie temperature, possibly linked to the ferroelectricity of the substrate [68]. If the temperature is further decreased, the samples undergo a superconducting transition at $T_c = 340, 255,$ and 300 mK for $y = 35, 45,$ and 67% , respectively. T_c is defined as the temperature at which the resistance is 50% of its value in the normal state (here at 800 mK). The transition temperature observed for the three samples is similar to that reported in the 2D electron system confined in standard SrTiO_3 substrates [11,60]. We note that a comparison between the phase diagram shown in Figure 1 and our data for the $\text{LaAlO}_3/\text{ST}({}^{18}\text{O}_y{}^{16}\text{O}_{1-y})_3$ interfaces is difficult due to the uncertainty on the equivalent 3D carrier density of the 2DES, which has an exponential charge profile inside the substrate. This pilot study shows that the presence of a ferroelectric SrTiO_3 substrate is compatible with the formation of a conducting—and even superconducting—system at the interface with LaAlO_3 , and opens the path to the exploration of its effect on the electronic properties.

6. Conclusions

SrTiO_3 plays host to a large variety of interesting physical phenomena. In particular, superconductivity can be obtained in the bulk and at a two-dimensional interface. Following the idea that superconductivity can be enhanced by ${}^{18}\text{O}$ substitution in SrTiO_3 we studied the properties of $\text{LaAlO}_3/\text{SrTi}({}^{18}\text{O}_y{}^{16}\text{O}_{1-y})_3$ heterostructures with different ${}^{18}\text{O}$ concentrations (35%, 45%, and 67%) in the SrTiO_3 substrate. The observation of superconductivity at the interface of LaAlO_3 and isotope substituted SrTiO_3 with T_c on the order of 300 mK demonstrates that it is experimentally possible to induce two-dimensional superconductivity in a ferroelectric-like environment. Further investigations with different levels of doping may reveal higher superconducting critical temperatures in this system that combines ferroelectricity, superconductivity and SrTiO_3 —the passions of K.A. Müller.

Author Contributions: Data curation, G.S., M.B., C.W.R. and A.W.; Formal analysis, G.S. and M.B.; Investigation, G.S., M.B., D.P., C.W.R., A.W., S.G. and E.G.; Supervision, S.G., E.G., D.v.d.M. and J.-M.T.; Writing—original draft, G.S., M.B., C.W.R., A.W., S.G., D.v.d.M. and J.-M.T.; Writing—review & editing, G.S., M.B., D.P., C.W.R., A.W., S.G., E.G., D.v.d.M. and J.-M.T. All authors have read and agreed to the published version of the manuscript.

Funding: This work was supported by the Swiss National Science Foundation through Division II (projects 200020-179155 and 200020-179157). The research leading to these results has received funding from the European Research Council under the European Union's Seventh Framework Program (FP7/2007-2013)/ERC Grant Agreement 319286 Q-MAC).

Acknowledgments: We would like to thank Jennifer Fowlie for providing useful comments on the manuscript.

Conflicts of Interest: The authors declare no conflict of interest.

References

1. Bednorz, J.G.; Müller, K.A. Perovskite-type oxides—The new approach to high- T_c superconductivity. *Rev. Mod. Phys.* **1988**, *60*, 585–600. [[CrossRef](#)]
2. Müller, K.A.; Burkard, H. SrTiO_3 : An intrinsic quantum paraelectric below 4 K. *Phys. Rev. B* **1979**, *19*, 3593–3602. [[CrossRef](#)]
3. Bednorz, J.G.; Müller, K.A. $\text{Sr}_{1-x}\text{Ca}_x\text{TiO}_3$: An XY Quantum Ferroelectric with Transition to Randomness. *Phys. Rev. Lett.* **1984**, *52*, 2289–2292. [[CrossRef](#)]
4. Itoh, M.; Wang, R.; Inaguma, Y.; Yamaguchi, T.; Shan, Y.J.; Nakamura, T. Ferroelectricity Induced by Oxygen Isotope Exchange in Strontium Titanate Perovskite. *Phys. Rev. Lett.* **1999**, *82*, 3540–3543. [[CrossRef](#)]
5. Haeni, J.H.; Irvin, P.; Chang, W.; Uecker, R.; Reiche, P.; Li, Y.L.; Choudhury, S.; Tian, W.; Hawley, M.E.; Craigo, B.; et al. Room-temperature ferroelectricity in strained SrTiO_3 . *Nature* **2004**, *430*, 758–761. [[CrossRef](#)]

6. Schooley, J.; Hosler, W.; Ambler, E.; Becker, J.; Cohen, M.; Koonce, C. Dependence of the Superconducting Transition Temperature on Carrier Concentration in Semiconducting SrTiO₃. *Phys. Rev. Lett.* **1965**, *14*, 305–307. [[CrossRef](#)]
7. Collignon, C.; Lin, X.; Rischau, C.W.; Fauqué, B.; Behnia, K. Metallicity and Superconductivity in Doped Strontium Titanate. *Ann. Rev. Condens. Matter Phys.* **2019**, *10*, 25–44. [[CrossRef](#)]
8. Kan, D.; Terashima, T.; Kanda, R.; Masuno, A.; Tanaka, K.; Chu, S.; Kan, H.; Ishizumi, A.; Kanemitsu, Y.; Shimakawa, Y.; et al. Blue-light emission at room temperature from Ar⁺-irradiated SrTiO₃. *Nat. Mater.* **2005**, *4*, 816–819. [[CrossRef](#)]
9. Wrighton, M.S.; Ellis, A.B.; Wolczanski, P.T.; Morse, D.L.; Abrahamson, H.B.; Ginley, D.S. Strontium titanate photoelectrodes. Efficient photoassisted electrolysis of water at zero applied potential. *J. Am. Chem. Soc.* **1976**, *98*, 2774–2779. [[CrossRef](#)]
10. Ohtomo, A.; Hwang, H.Y. A high-mobility electron gas at the LaAlO₃/SrTiO₃ heterointerface. *Nature* **2004**, *427*, 423–426. [[CrossRef](#)]
11. Reyren, N.; Thiel, S.; Cavaglia, A.D.; Kourkoutis, L.F.; Hammerl, G.; Richter, C.; Schneider, C.W.; Kopp, T.; Ruetschi, A.S.; Jaccard, D.; et al. Superconducting Interfaces Between Insulating Oxides. *Science* **2007**, *317*, 1196–1199. [[CrossRef](#)]
12. Goodenough, J.B. Electronic and ionic transport properties and other physical aspects of perovskites. *Rep. Prog. Phys.* **2004**, *67*, 1915–1993. [[CrossRef](#)]
13. Müller, K.A.; Berlinger, W.; Waldner, F. Characteristic Structural Phase Transition in Perovskite-Type Compounds. *Phys. Rev. Lett.* **1968**, *21*, 814–817. [[CrossRef](#)]
14. Cowley, R.A. Lattice Dynamics and Phase Transitions of Strontium Titanate. *Phys. Rev.* **1964**, *134*, A981–A997. [[CrossRef](#)]
15. Zhong, W.; Vanderbilt, D. Effect of quantum fluctuations on structural phase transitions in SrTiO₃ and BaTiO₃. *Phys. Rev. B* **1996**, *53*, 5047–5050. [[CrossRef](#)] [[PubMed](#)]
16. Burke, W.J.; Pressley, R.J. Stress induced ferroelectricity in SrTiO₃. *Solid State Commun.* **1971**, *9*, 191–195. [[CrossRef](#)]
17. Uwe, H.; Sakudo, T. Stress-induced ferroelectricity and soft phonon modes in SrTiO₃. *Phys. Rev. B* **1976**, *13*, 271–286. [[CrossRef](#)]
18. Mishra, S.K.; Ranjan, R.; Pandey, D.; Ranson, P.; Ouillon, R.; Pinan-Lucarre, J.-P.; Pruzan, P. A combined X-ray diffraction and Raman scattering study of the phase transitions in Sr_{1-x}Ca_xTiO₃ (x = 0.04, 0.06, and 0.012). *J. Solid State Chem.* **2005**, *178*, 2846–2857. [[CrossRef](#)]
19. Spinelli, A.; Torija, M.A.; Liu, C.; Jan, C.; Leighton, C. Electronic transport in doped SrTiO₃: Conduction mechanisms and potential applications. *Phys. Rev. B* **2010**, *81*, 155110. [[CrossRef](#)]
20. Ohta, S.; Nomura, T.; Ohta, H.; Koumoto, K. High-temperature carrier transport and thermoelectric properties of heavily La- or Nb-doped SrTiO₃ single crystals. *J. Appl. Phys.* **2005**, *97*, 034106. [[CrossRef](#)]
21. Tufte, O.; Chapman, P. Electron Mobility in Semiconducting Strontium Titanate. *Phys. Rev.* **1967**, *155*, 796–802. [[CrossRef](#)]
22. van der Marel, D.; van Mechelen, J.L.M.; Mazin, I.I. Common Fermi-liquid origin of T² resistivity and superconductivity in n-type SrTiO₃. *Phys. Rev. B* **2011**, *84*, 205111. [[CrossRef](#)]
23. Gregory, B.; Arthur, J.; Seidel, G. Measurements of the Fermi surface of SrTiO₃:Nb. *Phys. Rev. B* **1979**, *19*, 1039–1048. [[CrossRef](#)]
24. Lin, X.; Bridoux, G.; Gourgout, A.; Seyfarth, G.; Krämer, S.; Nardone, M.; Fauqué, B.; Behnia, K. Critical Doping for the Onset of a Two-Band Superconducting Ground State in SrTiO₃. *Phys. Rev. Lett.* **2014**, *112*, 207002. [[CrossRef](#)]
25. Schooley, J.F.; Hosler, W.R.; Cohen, M.L. Superconductivity in Semiconducting SrTiO₃. *Phys. Rev. Lett.* **1964**, *12*, 474–475. [[CrossRef](#)]
26. Koonce, C.S.; Cohen, M.L.; Schooley, J.F.; Hosler, W.R.; Pfeiffer, E.R. Superconducting Transition Temperatures of Semiconducting SrTiO₃. *Phys. Rev.* **1967**, *163*, 380–390. [[CrossRef](#)]
27. Appel, J. Soft-Mode Superconductivity in SrTiO_{3-x}. *Phys. Rev.* **1969**, *180*, 508–516. [[CrossRef](#)]
28. Bussmann-Holder, A.; Simon, A.; Büttner, H. Possibility of a common origin to ferroelectricity and superconductivity in oxides. *Phys. Rev. B* **1989**, *39*, 207–214. [[CrossRef](#)]

29. Edge, J.M.; Kedem, Y.; Aschauer, U.; Spaldin, N.A.; Balatsky, A.V. Quantum Critical Origin of the Superconducting Dome in SrTiO₃. *Phys. Rev. Lett.* **2015**, *115*, 247002. [[CrossRef](#)]
30. Kahn, A.H.; Leyendecker, A.J. Electronic Energy Bands in Strontium Titanate. *Phys. Rev.* **1964**, *135*, A1321–A1325. [[CrossRef](#)]
31. Cohen, M.L. Superconductivity in Many-Valley Semiconductors and in Semimetals. *Phys. Rev.* **1964**, *134*, A511–A521. [[CrossRef](#)]
32. Mattheiss, L.F. Energy Bands for KNiF₃, SrTiO₃, KMoO₃, and KTaO₃. *Phys. Rev. B* **1972**, *6*, 4718–4740. [[CrossRef](#)]
33. Binnig, G.; Baratoff, A.; Hoenig, H.E.; Bednorz, J.G. Two-Band Superconductivity in Nb-Doped SrTiO₃. *Phys. Rev. Lett.* **1980**, *45*, 1352–1355. [[CrossRef](#)]
34. van Mechelen, J.L.M.; van der Marel, D.; Grimaldi, C.; Kuzmenko, A.B.; Armitage, N.P.; Reyren, N.; Hagemann, H.; Mazin, I.I. Electron-Phonon Interaction and Charge Carrier Mass Enhancement in SrTiO₃. *Phys. Rev. Lett.* **2008**, *100*, 226403. [[CrossRef](#)]
35. McCalla, E.; Gastiasoro, M.N.; Cassuto, G.; Fernandes, R.M.; Leighton, C. Low-temperature specific heat of doped SrTiO₃: Doping dependence of the effective mass and Kadowaki-Woods scaling violation. *Phys. Rev. Mater.* **2019**, *3*, 022001. [[CrossRef](#)]
36. Devreese, J.T.; Klimin, S.N.; van Mechelen, J.L.M.; van der Marel, D. Many-body large polaron optical conductivity in SrTi_{1-x}Nb_xO₃. *Phys. Rev. B* **2010**, *81*, 125119. [[CrossRef](#)]
37. Eagles, D.M. Possible Pairing without Superconductivity at Low Carrier Concentrations in Bulk and Thin-Film Superconducting Semiconductors. *Phys. Rev.* **1969**, *186*, 456–463. [[CrossRef](#)]
38. Ngai, K.L. Two-Phonon Deformation Potential and Superconductivity in Degenerate Semiconductors. *Phys. Rev. Lett.* **1974**, *32*, 215–218. [[CrossRef](#)]
39. Gor'kov, L.P. Phonon mechanism in the most dilute superconductor n-type SrTiO₃. *Proc. Natl. Acad. Sci. USA* **2016**, *113*, 4646–4651. [[CrossRef](#)]
40. Klimin, S.N.; Tempere, J.; van der Marel, D.; Devreese, J.T. Microscopic mechanisms for the Fermi-liquid behavior of Nb-doped strontium titanate. *Phys. Rev. B* **2012**, *86*, 045113. [[CrossRef](#)]
41. Enderlein, C.; Ferreira de Oliveira, J.; Tompsett, D.A.; Baggio Saitovitch, E.; Saxena, S.S.; Lonzarich, G.G.; Rowley, S.E. Superconductivity mediated by polar modes in ferroelectric metals. *Nat. Commun.* **2020**, *11*, 4852. [[CrossRef](#)] [[PubMed](#)]
42. Jarlborg, T. Tuning of the electronic screening and electron-phonon coupling in doped SrTiO₃ and WO₃. *Phys. Rev. B* **2000**, *61*, 9887–9890. [[CrossRef](#)]
43. Rowley, S.E.; Spalek, L.J.; Smith, R.P.; Dean, M.P.M.; Itoh, M.; Scott, J.F.; Lonzarich, G.G.; Saxena, S.S. Ferroelectric quantum criticality. *Nat. Phys.* **2014**, *10*, 367. [[CrossRef](#)]
44. Stucky, A.; Scheerer, G.W.; Ren, Z.; Jaccard, D.; Poumirol, J.M.; Barreateau, C.; Giannini, E.; van der Marel, D. Isotope effect in superconducting n-doped SrTiO₃. *Sci. Rep.* **2016**, *6*, 37582. [[CrossRef](#)]
45. Tomioka, Y.; Shirakawa, N.; Shibuya, K.; Inoue, I.H. Enhanced superconductivity close to a non-magnetic quantum critical point in electron-doped strontium titanate. *Nat. Commun.* **2019**, *10*, 738. [[CrossRef](#)]
46. Rischau, C.W.; Lin, X.; Grams, C.P.; Finck, D.; Harms, S.; Engelmayer, J.; Lorenz, T.; Gallais, Y.; Fauqué, B.; Hemberger, J.; et al. A ferroelectric quantum phase transition inside the superconducting dome of Sr_{1-x}Ca_xTiO_{3-δ}. *Nat. Phys.* **2017**, *13*, 643. [[CrossRef](#)]
47. Ruhman, J.; Lee, P.A. Superconductivity at very low density: The case of strontium titanate. *Phys. Rev. B* **2016**, *94*, 224515. [[CrossRef](#)]
48. Bussmann-Holder, A.; Bishop, A.R.; Simon, A. Enhancement of T_c in BCS theory extended by interband two-phonon exchange. *Z. Phys. B Condens. Matter* **1993**, *90*, 183–186. [[CrossRef](#)]
49. van der Marel, D.; Barantani, F.; Rischau, C.W. Possible mechanism for superconductivity in doped SrTiO₃. *Phys. Rev. Res.* **2019**, *1*, 013003. [[CrossRef](#)]
50. Santander-Syro, A.F.; Copie, O.; Kondo, T.; Fortuna, F.; Pailhes, S.; Weht, R.; Qiu, X.G.; Bertran, F.; Nicolaou, A.; Taleb-Ibrahimi, A.; et al. Two-dimensional electron gas with universal subbands at the surface of SrTiO₃. *Nature* **2011**, *469*, 189–193. [[CrossRef](#)]

51. Meevasana, W.; King, P.D.C.; He, R.H.; Mo, S.K.; Hashimoto, M.; Tamai, A.; Songsiririthigul, P.; Baumberger, F.; Shen, Z.X. Creation and control of a two-dimensional electron liquid at the bare SrTiO₃ surface. *Nat. Mater.* **2011**, *10*, 114–118. [[CrossRef](#)]
52. Kim, M.; Kozuka, Y.; Bell, C.; Hikita, Y.; Hwang, H.Y. Intrinsic spin-orbit coupling in superconducting δ -doped SrTiO₃ heterostructures. *Phys. Rev. B* **2012**, *86*, 085121. [[CrossRef](#)]
53. Thiel, S.; Hammerl, G.; Schmehl, A.; Schneider, C.W.; Mannhart, J. Tunable Quasi-Two-Dimensional Electron Gases in Oxide Heterostructures. *Science* **2006**, *313*, 1942–1945. [[CrossRef](#)]
54. Bristowe, N.C.; Ghosez, P.; Littlewood, P.B.; Artacho, E. The origin of two-dimensional electron gases at oxide interfaces: insights from theory. *J. Phys. Condens. Matter* **2014**, *26*, 143201. [[CrossRef](#)]
55. Yu, L.; Zunger, A. A polarity-induced defect mechanism for conductivity and magnetism at polar-nonpolar oxide interfaces. *Nat. Commun.* **2014**, *5*, 5118. [[CrossRef](#)]
56. Tinkham, M. Effect of Fluxoid Quantization on Transitions of Superconducting Films. *Phys. Rev.* **1963**, *129*, 2413–2422. [[CrossRef](#)]
57. Reyren, N.; Gariglio, S.; Caviglia, A.D.; Jaccard, D.; Schneider, T.; Triscone, J.M. Anisotropy of the superconducting transport properties of the LaAlO₃/SrTiO₃ interface. *Appl. Phys. Lett.* **2009**, *94*, 112506. [[CrossRef](#)]
58. Ben Shalom, M.; Sachs, M.; Rakhmilevitch, D.; Palevski, A.; Dagan, Y. Tuning Spin-Orbit Coupling and Superconductivity at the SrTiO₃/LaAlO₃ Interface: A Magnetotransport Study. *Phys. Rev. Lett.* **2010**, *104*, 126802. [[CrossRef](#)] [[PubMed](#)]
59. Gariglio, S.; Gabay, M.; Mannhart, J.; Triscone, J.M. Interface superconductivity. *Phys. C Superconduct. Appl.* **2015**, *514*, 189–198. [[CrossRef](#)]
60. Caviglia, A.D.; Gariglio, S.; Reyren, N.; Jaccard, D.; Schneider, T.; Gabay, M.; Thiel, S.; Hammerl, G.; Mannhart, J.; Triscone, J.M. Electric field control of the LaAlO₃/SrTiO₃ interface ground state. *Nature* **2008**, *456*, 624–627. [[CrossRef](#)]
61. Gariglio, S.; Gabay, M.; Triscone, J.M. Research Update: Conductivity and beyond at the LaAlO₃/SrTiO₃ interface. *APL Mater.* **2016**, *4*, 060701. [[CrossRef](#)]
62. Cancellieri, C.; Reyren, N.; Gariglio, S.; Caviglia, A.D.; Fete, A.; Triscone, J.M. Influence of the growth conditions on the LaAlO₃/SrTiO₃ interface electronic properties. *EPL (Europhys. Lett.)* **2010**, *91*, 17004. [[CrossRef](#)]
63. Gariglio, S.; Reyren, N.; Caviglia, A.D.; Triscone, J.M. Superconductivity at the LaAlO₃/SrTiO₃ interface. *J. Phys. Condens. Matter* **2009**, *21*, 164213. [[CrossRef](#)]
64. Unoki, H.; Sakudo, T. Electron Spin Resonance of Fe³⁺ in SrTiO₃ with Special Reference to the 110° K Phase Transition. *J. Phys. Soc. Jpn* **1967**, *23*, 546–552. [[CrossRef](#)]
65. Shirane, G.; Yamada, Y. Lattice-Dynamical Study of the 110° K Phase Transition in SrTiO₃. *Phys. Rev.* **1969**, *177*, 858–863. [[CrossRef](#)]
66. Tao, Q.; Loret, B.; Xu, B.; Yang, X.; Rischau, C.W.; Lin, X.; Fauqué, B.; Verstraete, M.J.; Behnia, K. Nonmonotonic anisotropy in charge conduction induced by antiferrodistortive transition in metallic SrTiO₃. *Phys. Rev. B* **2016**, *94*, 035111. [[CrossRef](#)]
67. Wang, J.; Yang, L.; Rischau, C.W.; Xu, Z.; Ren, Z.; Lorenz, T.; Lin, X.; Behnia, K. Charge transport in a polar metal. *npj Quantum Mater.* **2019**, *4*, 61. [[CrossRef](#)]
68. Tuvia, G.; Frenkel, Y.; Rout, P.K.; Silber, I.; Kalisky, B.; Dagan, Y. Ferroelectric Exchange Bias Affects Interfacial Electronic States. *Adv. Mater.* **2020**, *32*, 2000216. [[CrossRef](#)] [[PubMed](#)]

Publisher's Note: MDPI stays neutral with regard to jurisdictional claims in published maps and institutional affiliations.



© 2020 by the authors. Licensee MDPI, Basel, Switzerland. This article is an open access article distributed under the terms and conditions of the Creative Commons Attribution (CC BY) license (<http://creativecommons.org/licenses/by/4.0/>).